Acquired resistance to the TRK inhibitor entrectinib in colorectal cancer

Russo, Mariangela; Misale, Sandra; Wei, Ge; Siravegna, Giulia; Crisafulli, Giovanni; Lazzari, Luca; Corti, Giorgio; Rospo, Giuseppe; Novara, Luca; Mussolin, Benedetta; Bartolini, Alice; Cam, Nicholas; Patel, Roopal; Yan, Shunqi; Shoemaker, Robert; Wild, Robert; Di Nicolantonio, Federica; Sartore-Bianchi, Andrea; Li, Gang; Siena, Salvatore; Bardelli, Alberto.
Acquired resistance to the TRK inhibitor entrectinib in colorectal cancer.
CANCER DISCOVERY. 6 (1) pp: 36-44.
DOI: 10.1158/2159-8290.CD-15-0940

Acquired resistance to the TRK inhibitor entrectinib in colorectal cancer

Mariangela Russo[1,2,3]*, Sandra Misale[2]*, Ge Wei[4]*, Giulia Siravegna[1,2], Giovanni Crisafulli[2], Luca Lazzari[1,2], Giorgio Corti[2], Giuseppe Rospo[2], Luca Novara[2], Benedetta Mussolin[2], Alice Bartolini[2], Nicholas Cam[4], Roopal Patel[4], Shunqi Yan[4], Robert Shoemaker[4], Robert Wild[4], Federica Di Nicolantonio[1,2], Andrea Sartore Bianchi[5], Gang Li[4], Salvatore Siena[5,6,§], Alberto Bardelli[1,2,§,#]

[1]University of Torino, Department of Oncology, SP 142, Km 3.95, 10060 Candiolo, Torino, Italy; [2]Candiolo Cancer Institute – FPO, IRCCS, Candiolo, Torino, Italy; [3] FIRC Institute of Molecular Oncology (IFOM), Milano, Italy; [4] Ignyta, Inc. San Diego, CA, USA; [5]Department of Hematology and Oncology, Niguarda Cancer Center, Ospedale Niguarda Ca' Granda, Milan, Italy; [6]Università degli Studi di Milano, Milan, Italy

* Drs. Russo, Misale and Wei contributed equally to this article; § Drs. Bardelli and Siena are co-senior author; # Address correspondence to:
Alberto Bardelli at: alberto.bardelli@unito.it
University of Torino, Department of Oncology, FPO, IRCCS,
SP 142, Km 3.95, Candiolo (TO) , ZIP 10060 , Italy
Phone: +39-011-9933548

Running Title:

TRKA mutations and resistance to entrectinib in CRC

Key words:

Colorectal, acquired resistance, NTRK1, TRK inhibition, ctDNA

Conflict of interest

Ignyta co-authors are full time emplyees of Ignyta, and own Ignyta stocks. All the other authors do not have conflict of interest to declare.

Abstract

Entrectinib is a first-in-class pan-TRK kinase inhibitor currently undergoing clinical testing in colorectal cancer and other tumor types. A patient with metastatic colorectal cancer harboring an *LMNA-NTRK1* rearrangement displayed a remarkable response to treatment with entrectinib, which was followed by the emergence of resistance. To characterize the molecular bases of the patient's relapse, circulating tumor DNA (ctDNA) was collected longitudinally during treatment and a tissue biopsy, obtained before entrectinib treatment, was transplanted in mice (xenopatient), which then received the same entrectinib regimen until resistance developed. Genetic profiling of ctDNA and xeno-patient samples showed acquisition of two point mutations in the catalytic domain of *NTRK1*, p.G595R and p.G667C. Biochemical and pharmacological analysis in multiple preclinical models confirmed that either mutation renders the TRKA kinase insensitive to entrectinib. These findings can be immediately exploited to design next generation TRKA inhibitors.

Significance

We provide proof of principle that analyses of xenopatients (avatar) and liquid biopsies allow the identification of drug resistance mechanisms in parallel with clinical treatment of individual patient. We describe for the first time that p.G595R and p.G667C TRKA mutations drive acquired resistance to entrectinib in colorectal cancers carrying *NTRK1* rearrangements.

Introduction

TRK receptors are a family of tyrosine kinases that comprises three members: TRKA, TRKB and TRKC, encoded by the *NTRK1* (neurotrophic tyrosine kinase receptor, type 1), *NTRK2* and *NTRK3* genes, respectively. Genomic rearrangement is the most common mechanism of oncogenic activation for this family of receptors, resulting in sustained cancer cell proliferation through activation of MAPK and AKT downstream pathways (1). Rearrangements of the *NTRK1*, *NTRK2* and *NTRK3* genes occur across different tumors including colorectal cancers (CRCs) (2).

Entrectinib (RXDX-101, previously known as NMS-E628) is a potent pan-TRK, ALK, ROS1 inhibitor, currently undergoing phase I clinical trial(3). During treatment with entrectinib a patient with metastatic colorectal cancer harboring an *LMNA-NTRK1* rearrangement showed a remarkable response. We reasoned that, as it has been shown for most targeted agents, response to entrectinib might be limited in time due to the emergence of acquired resistance. Nothing is presently known on the mechanisms of resistance to entrectinib and consequently further lines of treatment are not available. We postulated that it might be possible to identify the resistance mechanism(s) while the patient was being treated by analyzing circulating tumor DNA (ctDNA) and developing a xenopatient (avatar).

Results

Acquired resistance to TRKA inhibition in a CRC patient.

A molecular screen identified a genetic rearrangement involving exon 10 of *NTRK1* and exon 11 of the *LMNA* genes(4) in a patient with metastatic colorectal cancer (mCRC) whose disease was intrinsically resistant to 1st line FOLFOX, 2nd line FOLFIRI/cetuximab and 3rd line Irinotecan. We and others have previously reported that CRC cell models harboring *NTRK1* translocations are sensitive to *NTRK1* silencing and to TRKA (protein encoded by *NTRK1* gene) kinase inhibition (5-7). Based on this, the patient was enrolled in the phase I ALKA clinical trial (EudraCT Number 2012-000148-88) of the pan-TRK kinase inhibitor entrectinib, a first-in-class drug currently undergoing clinical testing(3) . The patient received entrectinib on an intermittent dosing schedule of 4 days on/3 days off for three weeks followed by a week break in every 28-day cycle(4). Treatment was remarkably effective and well tolerated, leading to a partial response (PR) with 30% tumor shrinkage of multiple liver metastases that was demonstrated by an early CT scan assessment performed after 30 days of treatment. The clinical response lasted four months, followed by the emergence of drug resistance as evaluated by RECIST (Response Evaluation Criteria in Solid Tumor) progression (Fig. 1 upper panels).

Emergence of *NTRK1* mutations in ctDNA during entrectinib treatment

To unveil the molecular basis of acquired resistance to TRKA inhibition we analyzed circulating tumor DNA (ctDNA), a form of liquid biopsy (8) we

previously optimized to detect and monitor drug resistance in patients treated with targeted agents (9,10).

ctDNA extracted from plasma samples collected before treatment initiation and at clinical relapse was subjected to molecular profiling using the IRCC-TARGET panel, an NGS-platform based on 226 cancer related genes (10). Profiling of ctDNA at entrectinib resistance revealed two novel *NTRK1* genetic alterations in the kinase domain of the protein, p.G595R and p.G667C, which were not detected in ctDNA obtained before initiation of therapy (Supplementary Tables S1, S2). To monitor the *NTRK1* mutated alleles in the plasma of the patient collected through the treatment, droplet digital PCR (ddPCR) (11,12) assays were designed for both mutations. As a mean of tracking the overall disease, a ddPCR assay was also optimized to detect the *LMNA-NTRK1* rearrangement in ctDNA.

Longitudinal analysis of plasma revealed that the p.G595R and p.G667C mutated alleles were initially absent in ctDNA but emerged in the circulation as early as 4 weeks upon initiation of treatment with entrectinib (Fig. 1). *NTRK1* mutations frequencies continued to increase in ctDNA and peaked when clinical progression was radiologically confirmed (16 weeks after initiation of treatment). The profile of the *LMNA-NTRK1* rearrangement in ctDNA paralleled tumor response and resistance to entrectinib (Fig. 1; Supplementary Table S3).

Secondary resistance to entrectinib in CRC Xenopatient

To functionally evaluate the mechanistic basis of resistance to entrectinib, a biopsy specimen gathered before initiation of treatment was transplanted subcutaneously in an immunocompromised mouse (xenopatient) (see Supplementary Methods). Upon successful engraftment, the tumor was expanded in multiple mice, which were treated with dosage levels and schedules that matched clinically relevant exposure achievable in patients. Entrectinib induced remarkable tumor shrinkage in the xenopatient while vehicle treated tumors grew exponentially (Fig. 2A). After 3 weeks of drug dosing, one of the tumors treated with entrectinib rapidly developed resistance to TRKA inhibition (Fig. 2A). NGS-based molecular profiling of this resistant sample using the IRCC-TARGET panel unveiled the *LMNA-NTRK1* rearrangement peculiar of the patient and the *NTRK1* p.G595R mutation, which could not be detected in the untreated tumor (Supplementary Fig. S1A, B; Supplementary Tables S1, S2) .

Secondary resistance to entrectinib in cells carrying *NTRK1* rearrangements

To assess whether the mechanism of resistance was patient-specific or contingent on the peculiar *NTRK1* rearrangements, independent models of acquired resistance to entrectinib were established. The KM12 CRC cell line harbors a distinct genetic rearrangement involving exon 10 of *NTRK1* and exon 7 of *TPM3* gene (5,7) and is also highly sensitive to entrectinib (Fig. 2B,C). Independent batches of parental (sensitive) KM12 cells were exposed to either acute constant dose (R2) or escalating doses (R1) of entrectinib until resistant derivatives emerged (Fig. 2B,C) (see Supplementary Methods).

Molecular profiling of the cells that became resistant to lower concentrations of entrectinib (30-100 nM) (named KM12 R1) revealed the missense mutation p.G667C in the kinase domain of *NTRK1*, previously identified also in the plasma of the patient (Fig. 2B). When cells were made resistant to a higher doses (1-2 μM) of the drug (named KM12 R2), the *NTRK1* p.G595R alteration was detected (Fig. 2C). The experiment was repeated multiple times, the two mutations were never concomitantly detected in the same resistant populations indicating they occurred in independent cells.

To further evaluate the mechanisms of entrectinib resistance we engineered Ba/F3 cells to express ETV6-TRKA. In this model system the ETV6 domain mimics the dimerization effect of TRK fusion partners that occur in human tumors. Ba/F3 cells engineered to express ETV6-TRKA became exquisitely sensitive to entrectinib (Supplementary Fig.S2). ETV6-TRKA Ba/F3 cells were then exposed to entrectinib treatment until resistant derivatives emerged and analyzed as described above. Remarkably upon development of resistance Ba/F3 also acquired p.G595R mutation in the kinase domain of TRKA when a high dose of entrectinib was applied, while the p.G667C allele emerged in the presence of a lower dose of the drug (Supplementary Fig.S2). Analogously to what we observed in KM12, the two mutations were found in independent pools of Ba/F3 cells indicating they do not co-occur in the same cells.

NTRK1 p.G595R and p.G667C mutations drive resistance to TRK inhibitors

We then examined the impact of the p.G595R and p.G667C variants on the 3-dimensional (3D) structure of the TRKA catalytic domain (see Supplementary Methods). The binding model of entrectinib with wild type (WT) TRKA highlighted that entrectinib makes extensive hydrogen bonding as well as hydrophobic interactions with the protein in the ATP pocket where p.G595 and p.G667 residues are located (Fig. 3A). The p.G595R and p.G667C mutations create steric hindrance that either abrogates binding (p.G595R) or reduces the binding affinity (p.G667C) of entrectinib to the TRKA catalytic pocket (Fig. 3B,C respectively).

We next assessed whether and to what extent mutations in the kinase domain of *NTRK1* drive resistance to TRKA inhibition. We engineered Ba/F3 cells expressing wild type , p.G595R or p.G667C TPM3-TRKA fusion proteins. We then measured the sensitivity of *NTRK1* mutated cells to TRK inhibitors currently in clinical development. LOXO-101 is a TRK inhibitor in phase 1 trial for patients with advanced solid tumors with *NTRK* alterations (NCT02122913); TSR-011 is presently undergoing a phase 1 trial for patients with advanced solid tumors or lymphomas with *NTRK* alterations (NCT02048488).

As shown in Supplementary Fig.S3, Ba/F3 cells harboring the *NTRK1* translocation become highly sensitive to TRK inhibitors (Supplementary Fig. S3 A,B; Supplementary Table S4). On the contrary *NTRK1* p.G595R or p.G667C mutations are resistant to entrectinib, LOXO-101 and TSR-011 (Supplementary Fig. S3 C,D respectively). Of potential clinical relevance, and

in line with previous results, *NTRK1* p.G595R appears to be more potent in conferring resistance than p.G667C.

These results are indeed consistent with the observation that entrectinib and LOXO-101 retain a partial effect on p.G667C (IC_{50}=61 nM; IC50= 524nM respectively) but are totally ineffective on p.G595R (IC_{50}>1000 nM) in Ba/F3 engineered cells (Supplementary Table S4).

Alignment of the TRKA kinase domain with clinically targeted tyrosine kinases, such as ALK, ROS, EGFR, MET and KIT, showed that the glycine residues at position 595 and 667 lie in a conserved region (Supplementary Fig. S4A and S4B respectively), and are analogous to residues previously found to be associated with secondary resistance to other kinase inhibitors such as erlotinib, crizotinib and imatinib (Fig.3D,E respectively).

Biochemical characterization of *NTRK1* p.G595C and p.G667C in xenopatient derived cells.

To mechanistically study the impact of *NTRK1* resistant alleles, we established two cell lines, one from the xenopatient treated with vehicle, and the other from the xenopatient that became resistant to entrectinib (Fig. 4A). Both cell lines displayed the *LMNA-NTRK1* translocation found in the patient tumor (Figure 4B), but only cells derived from the xenotumor that had become resistant to entrectinib carried the p.G595R allele (Figure 4C). Both cell lines displayed a pharmacological response to entrectinib analogous to that observed in the corresponding xenopatients (Fig.4D). Biochemical

characterization confirmed that *NTRK1* secondary mutations render the corresponding proteins insensitive (or only marginally sensitive) to entrectinib and capable of activating downstream signaling in the presence of the drug (Fig. 4E, F). We next asked whether the tumor cell that had become resistant remained dependent on the expression of TRKA. Indeed, siRNA-mediated suppression of mutant *NTRK1* in resistant cells induced apoptosis, similarly to the knockdown of WT *NTRK1* in sensitive cells (Fig. 4G).

Discussion

A subset of CRCs carries *NTRK1* translocations, which also occur in other tumor types such as lung tumors and thyroid carcinomas (6,13-15). The TRK inhibitor entrectinib induced a remarkable clinical response in a patient with a metastatic colorectal cancer carrying a *LMNA-NTRK1* translocation, whose disease was intrinsically refractory to three prior lines of therapy including anti-EGFR inhibition(4) . However, after four months of treatment, resistance developed in this patient. The entrectinib half-life is 17-44h and the intermittent dosing regimen may have promoted or anticipated the development of resistance due to incomplete treatment coverage of the patient. Nevertheless, it is still unknown whether or not continuous dosing will affect the emergence and/or the type of acquired mutations.

In this work, we sought to identify mechanisms of resistance to entrectinib, as this is key to development of additional lines of therapy for patients carrying *NTRK1* rearrangements. The most commonly used approach to study

resistance to targeted therapies involves molecular profiling of tissue biopsy obtained at progression. However, tumor heterogeneity and tissue sampling limit the effectiveness of this strategy. In addition, tissues biopsies are not always feasible and are associated with non-negligible risks (16). Most importantly, even when the biopsy reveals emergence of alleles that were not present before treatment, their functional role in driving resistance remains to be formally established using functional assays. This requires significant experimental efforts, and the timeframe is not compatible with further treatment of the patient from whom the biopsy was obtained. We find that coupling pharmacological analyses of xenopatients with molecular profiles of liquid biopsies allows the identification of resistance mechanisms in parallel with clinical treatment of individual patients, thus potentially enabling decisions on following treatment options.

We report for the first time that acquisition of p.G595R and p.G667C mutations in the kinase domain of TRKA drive secondary resistance to TRK inhibition in CRC cells carrying *NTRK1* rearrangements. Both mutations were detected in patient plasma obtained at progression, suggesting that both are indeed associated with acquired resistance to entrectinib in the clinical setting. We found a remarkable concordance among results obtained in clinical samples and preclinical models. Genomic profiling of patient derived samples and multiple cell models pointed to the p.G595R or p.G667C *NTRK1* mutations as the only common mechanism of resistance to entrectinib.

Analysis of a larger number of patients will ultimately be needed to determine the clinical impact of the findings. Based on data obtained with other anticancer therapies based on kinase inhibitors, it is possible that other mechanisms of resistance to entrectinib could occur, including activation of parallel pathways able to bypass TRKA inhibition.

Interestingly, we found that the emergence of each of the two mutations might be dependent on the entrectinib concentration used. *NTRK1* p.G667C emerged when cells were exposed to a low concentration of the inhibitor, while it was absent from cells made resistant to higher dose.

Structural model-based characterization also indicates that the potency of the p.G667C mutation in conferring resistance to entrectinb is weaker than p.G595R. Both mutations fall in the ATP binding pocket and are analogous to resistance mutations which have been described for other clinically druggable tyrosine kinase fusions. While p.G595C completely abrogates the binding of entrectinib to TRKA, the p.G667C only reduces affinity of binding. In line with this, homology alignment showed that TRKA p.G595R is analogous to ALK p.G1202R, while TRKA p.G667C to ALK p.G1269A. As for ALK p.G1269A which mediates resistance to crizotinib, this alteration can be overcome with second generation ALK inhibitors, such as ceritinib and alectinib, while both are ineffective on ALK p.G1202R(17-19); entrectinib at clinically achievable exposure still retain a partial effect on p.G667C but not on p.G595R TRKA.

Of note, while we found that cells that develop entrectinib's resistance remain dependent on the expression of TRKA, none of the TRK inhibitors current being tested in the clinic (LOXO-101 and TSR-011) can overcome resistance

driven by p.G595R. Accordingly, the biochemical and pharmacological characterization of the preclinical models described here highlight the need of developing next generation TRKA inhibitors that do not rely on specific spatial accommodation of the drug-target interaction around G595 region, aimed at overcoming resistance driven by the p.G595R variant.

In addition to providing clues for the development of second generation TRK inhibitors, our finding offer means of tracking –non invasively- the emergence of resistance to entrectinib. Monitoring of *NTRK1* resistant variants (p.G595R and p.G667C) in the plasma of patients treated with entrectinib could be valuable to predict recurrences.

Material and Methods

Cells lines authentication

KM12 CRC cells were obtained from NCI60 cell line bank and authenticated in May 2011. The genetic identity of cell line was last checked no less than three months before performing experiments by Cell ID™ System and by Gene Print® 10 System (Promega), throught Short Tandem Repeats (STR) at 10 different loci (D5S818, D13S317, D7S820, D16S539, D21S11, vWA, TH01, TPOX, CSF1PO and amelogenin). Amplicons from multiplex PCRs were separated by capillary electrophoresis (3730 DNA Analyzer, Applied Biosystems) and analyzed using GeneMapperID software from Life

Technologies. Cell lines were tested and resulted negative for mycoplasma contamination with Venor GeM Classic Kit (Minerva Biolabs).

Establishment of primary colorectal cancer cell line

Primary colorectal cancer cell lines were established from tumor tissues obtained from patient-derived xenografts. Tumor tissues were dissociated into single-cell suspension by mechanical dissociation using the gentleMACS Dissociator (Miltenyi Biotec) and enzymatic degradation of the extracellular matrix using the Tumor Dissociation Kit (Miltenyi Biotec) according to manufacturer's instructions. The cell suspension was then centrifuged at 1200 rpm for 5 minutes. Supernatants were removed and cell pellets were resuspended with DMEM/F12 medium containing 10% FBS. This process was repeated 3 times. Then, cell suspensions were filtered through a 70µm cell strainer (Falcon) and resuspended with culture media DMEM-F12 containing 2 mM L-glutamine, antibiotics (100 U/mL penicillin and 100 µg/mL streptomycin), gentamicin 50 µg/ml and 10 µM ROCK inhibitor Y-27632 (Selleck Chemicals Inc.).

Ba/F3-TPM3-TRKA WT , G595R and G667C generation

To generate Ba/F3 cells expressing TPM3-TRKA WT, TPM3-TRKA G595R and TPM3-TRKA G667C the cDNAs were cloned from KM12 cells by RT-PCR and inserted into a lentiviral vector pVL-EF1a-MCS-IRES-Puro (BioSettia, San Diego, CA). After confirmation by direct sequencing, VSVG-pseudo-typed lentiviruses were introduced into the murine IL-3 dependent pro-B cell Ba/F3. The transduced Ba/F3 cells were selected at 1 µg/mL of

puromycin in the murine IL-3 containing RPMI and 10% FBS media for two weeks. The stable cell pools were further selected in RPMI and 10% FBS media without murine IL-3 for 4 weeks.

Drugs

Entrectinib, LOXO-101(20) and TSR-011(21) were obtained from Ignyta, San Diego (CA, USA).

Patient's samples collection

Patient's plasma and tumor biopsy were obtained through protocols approved by local Ethical Committee at Ospedale Niguarda Ca ' Granda, Milano, Italy. The study was conducted according to the provisions of the Declaration of Helsinki, and patient signed and provided his/her informed consent before sample collection. The liver biopsy was subcutaneously implanted in NOD-SCID mouse and experiments were performed according to a study protocol approved by Ethical Committee at Ospedale Niguarda Ca ' Granda, Milano, Italy.

Droplet digital PCR analysis

Isolated circulating free DNA was amplified using ddPCR™ Supermix for Probes (Bio-Rad) with *LMNA-NTRK1* translocation, *NTRK1* p.G595R and *NTRK1* p.G667C assays (sequences of custom designed probes are listed in Supplementary Table S5). ddPCR was then performed according to manufacturer's protocol and the results reported as percentage or fractional abundance of mutant DNA alleles to total (mutant plus wild type) DNA alleles.

8–10 µl of DNA template was added to 10 µl of ddPCR Supermix for Probes (Bio-Rad) and 2 µl of the primer and probe mixture. This reaction mix was added to a DG8 cartridge together with 60 µl of Droplet Generation Oil for Probes (Bio-Rad) and used for droplet generation. Droplets were then transferred to a 96-well plate (Eppendorf) and then thermal cycled with the following conditions: 5 min at 95 °C, 40 cycles of 94 °C for 30 s, 55 °C for 1 min followed by 98 °C for 10 min (Ramp Rate 2 °C/s). Droplets were analyzed with the QX200 Droplet Reader (Bio-Rad) for fluorescent measurement of FAM and HEX probes. Gating was performed based on positive and negative controls, and mutant populations were identified. The ddPCR data were analyzed with QuantaSoft analysis software (Bio-Rad) to obtain fractional abundance of the mutated alleles in the wild-type or normal background. The quantification of the target molecule was presented as number of total copies (mutant plus WT) per sample in each reaction. The number of positive and negative droplets is used to calculate the concentration of the target and reference DNA sequences and their Poisson-based 95% confidence intervals, as previously shown(22). ddPCR analysis of normal control plasma DNA (from cell lines) and no DNA template controls were always included. Samples with too low positive events were repeated at least twice in independent experiments to validate the obtained results.

Next Generation Sequencing analysis

Libraries were prepared with Nextera Rapid Capture Custom Enrichment Kit (Illumina Inc., San Diego, CA, USA), according to the manufacturer's protocol. Preparation of libraries was performed using up to 150ng of plasma ctDNA

and 100 ng of gDNA from both cells and avatar fresh tissue. gDNA was fragmented using transposons, adding simultaneously adapter sequences. For ctDNA libraries preparation was used NEBNext® Ultra™ DNA Library Prep Kit for Illumina® (New England BioLabs Inc., Ipswich MA), with optimized protocol. Purified gDNA after the tagmentation step, and ctDNA were used as template for subsequent PCR to introduce unique sample barcodes. Fragments' size distribution of the DNA was assessed using the 2100 Bioanalyzer with a High Sensitivity DNA assay kit (Agilent Technologies, Santa Clara, CA). Equal amount of DNA libraries were pooled and subjected to targeted panel hybridization capture. Libraries were then sequenced using Illumina MiSeq sequencer (Illumina Inc., San Diego, CA, USA).

Bioinformatic analysis

FastQ files generated by Illumina sequencer were mapped to the human reference (assembly hg19) using BWA-mem algorithm(23); PCR duplicates were then removed using the SAMtools package(24). Xenome software(25) was applied to remove murine sequences from xenopatient samples prior to alignment. We used a custom script pipeline for NGS in order to call somatic variations when supported by at least 1.5% allelic frequency and 5% significance level obtained with a Fisher's Test. Mutational analyses were the result of comparison between pre- and post-treatment samples.

Detection of *LMNA-NTRK1* rearrangement in ctDNA

ctDNA obtained from blood draw collected before entrectinib treatment started was analyzed by NGS as described above. To unveil the specific *LMNA*-

NTRK1 genetic rearrangement, a combination of BWA (v. 0.7.10) and BLAT (v. 35) was used. BWA was first used to align reads to the hg19 human reference genome with default options. The reads with a non perfect alignment from BWA, potentially containing translocations, were extracted and aligned using BLAT (tileSize 11 and stepSize 5). The resulting PSL alignment was then post-processed to detect chimeric alignments. Gene fusion calling was performed using the following criteria: i) each fusion partner must have at least 25 mapped bases on the respective end of the read; ii) the fusion partners must map to two different genes; iii) each reported fusion breakpoint must be supported by at least 10 reads. Based on the fusion sequence identified by NGS analysis, specific ddPCR primers and probes for the *LMNA-NTRK1* rearrangement were designed using Primer3 Input (version 0.4.0) following BioRad instructions available on the website. Primers and probes sequences are listed in Supplementary Table S5.

Kinase domain alignment

The aminoacidic sequences of human TRKA [P04629], ALK [Q9UM73], ROS1 [P08922], EGFR [P00533], KIT [P10721] and MET [P08581] were obtained from UniprotKB database (26). Their kinase domains were aligned using the MUSCLE tool (27) and results were post-processed using Jalview (28).

Acknowledgments

Supported by the European Community's Seventh Framework Programme under grant agreement no. 602901, MErCuRIC (A.B.); Innovative Medicines Initiative grant no.115749, CANCER-ID (A.B.) Associazione Italiana per la Ricerca sul Cancro (AIRC) IG grant no. 12812 (A.B.); AIRC 2010 Special Program Molecular Clinical Oncology 5 per mille, project no. 9970 (A.B.); FPRC 5 per mille 2010 and 2011 Ministero della Salute (F.D.N. and A.B.); Ministero dell'Istruzione, dell'Università e della Ricerca, progetto PRIN (A.B.). Investigators at Niguarda Cancer Center (ASB, SS) are also supported by Fondazione Oncologia Niguarda Onlus.

References

1. Vaishnavi A, Le AT, Doebele RC. TRKing down an old oncogene in a new era of targeted therapy. Cancer Discov 2015;5(1):25-34.
2. Shaw AT, Hsu PP, Awad MM, Engelman JA. Tyrosine kinase gene rearrangements in epithelial malignancies. Nat Rev Cancer 2013;13(11):772-87.
3. Siena S, Drilon AE, Ou S-HI, Farago AF, Patel M, Bauer TM, et al. Entrectinib (RXDX-101), an oral pan-Trk, ROS1, and ALK inhibitor in patients with advanced solid tumors harboring gene rearrangements. European Journal of Cancer 2015;50:Supplement 3.
4. Sartore-Bianchi A, Ardini E, Bosotti R, Amatu A, Valtorta E, Somaschini A, et al. Sensitivity to Entrectinib Associated With a Novel LMNA-NTRK1 Gene Fusion in Metastatic Colorectal Cancer. J Natl Cancer Int 2016;108. [Epub ahead of print].
5. Ardini E, Bosotti R, Borgia AL, De Ponti C, Somaschini A, Cammarota R, et al. The TPM3-NTRK1 rearrangement is a recurring event in colorectal carcinoma and is associated with tumor sensitivity to TRKA kinase inhibition. Mol Oncol 2014;8(8):1495-507.
6. Vaishnavi A, Capelletti M, Le AT, Kako S, Butaney M, Ercan D, et al. Oncogenic and drug-sensitive NTRK1 rearrangements in lung cancer. Nat Med 2013;19(11):1469-72.
7. Medico E, Russo M, Picco G, Cancelliere C, Valtorta E, Corti G, et al. The molecular landscape of colorectal cancer cell lines unveils clinically actionable kinase targets. Nat Commun 2015;6:7002.
8. Siravegna G, Bardelli A. Genotyping cell-free tumor DNA in the blood to detect residual disease and drug resistance. Genome Biol 2014;15(8):449.

9. Misale S, Yaeger R, Hobor S, Scala E, Janakiraman M, Liska D, et al. Emergence of KRAS mutations and acquired resistance to anti-EGFR therapy in colorectal cancer. Nature 2012;486(7404):532-6.
10. Siravegna G, Mussolin B, Buscarino M, Corti G, Cassingena A, Crisafulli G, et al. Clonal evolution and resistance to EGFR blockade in the blood of colorectal cancer patients. Nat Med 2015;21(7):795-801.
11. Hindson BJ, Ness KD, Masquelier DA, Belgrader P, Heredia NJ, Makarewicz AJ, et al. High-throughput droplet digital PCR system for absolute quantitation of DNA copy number. Anal Chem 2011;83(22):8604-10.
12. Reinert T, Schøler LV, Thomsen R, Tobiasen H, Vang S, Nordentoft I, et al. Analysis of circulating tumour DNA to monitor disease burden following colorectal cancer surgery. Gut 2015. [Epub ahead of print]
13. Stransky N, Cerami E, Schalm S, Kim JL, Lengauer C. The landscape of kinase fusions in cancer. Nat Commun 2014;5:4846.
14. Wiesner T, He J, Yelensky R, Esteve-Puig R, Botton T, Yeh I, et al. Kinase fusions are frequent in Spitz tumours and spitzoid melanomas. Nat Commun 2014;5:3116.
15. Bounacer A, Schlumberger M, Wicker R, Du-Villard JA, Caillou B, Sarasin A, et al. Search for NTRK1 proto-oncogene rearrangements in human thyroid tumours originated after therapeutic radiation. Br J Cancer 2000;82(2):308-14.
16. Overman MJ, Modak J, Kopetz S, Murthy R, Yao JC, Hicks ME, et al. Use of research biopsies in clinical trials: are risks and benefits adequately discussed? J Clin Oncol 2013;31(1):17-22.
17. Friboulet L, Li N, Katayama R, Lee CC, Gainor JF, Crystal AS, et al. The ALK inhibitor ceritinib overcomes crizotinib resistance in non-small cell lung cancer. Cancer Discov 2014;4(6):662-73.
18. Katayama R, Friboulet L, Koike S, Lockerman EL, Khan TM, Gainor JF, et al. Two novel ALK mutations mediate acquired resistance to the next-generation ALK inhibitor alectinib. Clin Cancer Res 2014;20(22):5686-96.
19. Zou HY, Friboulet L, Kodack DP, Engstrom LD, Li Q, West M, et al. PF-06463922, an ALK/ROS1 Inhibitor, Overcomes Resistance to First and Second Generation ALK Inhibitors in Preclinical Models. Cancer Cell 2015;28(1):70-81.
20. Doebele RC, Davis LE, Vaishnavi A, Le AT, Estrada-Bernal A, Keysar S, et al. An Oncogenic NTRK Fusion in a Patient with Soft-Tissue Sarcoma with Response to the Tropomyosin-Related Kinase Inhibitor LOXO-101. Cancer Discov 2015;5(10):1049-57.
21. Wilcoxen KM, inventor; Tesaro, Inc., assignee. Modulating certain tyrosine kinases. United States patent US wo2013074518a1. 2013 May 23.
22. Hayden RT, Gu Z, Ingersoll J, Abdul-Ali D, Shi L, Pounds S, et al. Comparison of droplet digital PCR to real-time PCR for quantitative detection of cytomegalovirus. J Clin Microbiol 2013;51(2):540-6.
23. Li H, Durbin R. Fast and accurate long-read alignment with Burrows-Wheeler transform. Bioinformatics 2010;26(5):589-95.
24. Li H, Handsaker B, Wysoker A, Fennell T, Ruan J, Homer N, et al. The Sequence Alignment/Map format and SAMtools. Bioinformatics 2009;25(16):2078-9.

25. Conway T, Wazny J, Bromage A, Tymms M, Sooraj D, Williams ED, et al. Xenome--a tool for classifying reads from xenograft samples. Bioinformatics 2012;28(12):i172-8.
26. Wu CH, Apweiler R, Bairoch A, Natale DA, Barker WC, Boeckmann B, et al. The Universal Protein Resource (UniProt): an expanding universe of protein information. Nucleic Acids Res 2006;34(Database issue):D187-91.
27. Edgar RC. MUSCLE: a multiple sequence alignment method with reduced time and space complexity. BMC Bioinformatics 2004;5:113.
28. Waterhouse AM, Procter JB, Martin DM, Clamp M, Barton GJ. Jalview Version 2--a multiple sequence alignment editor and analysis workbench. Bioinformatics 2009;25(9):1189-91.

Figure Legends

Figure 1. Tracking resistance to TRKA inhibition in ctDNA of a CRC patient.

CT scans of a patient with metastatic colorectal cancer harboring an *LMNA-NTRK1* rearrangement were recorded at baseline (March 2014), at the time of partial response to pan-TRK inhibitor entrectinib (April 2014) and upon disease progression (July 2014) (upper panels). Longitudinal analysis of plasma ctDNA collected at different time points throughout the treatment is shown in the lower panel. Red bars indicate absolute *LMNA-NTRK1* copies in 1 ml of plasma; blue and black lines represent *NTRK1* p.G595R and p.G667C mutated alleles (%), respectively. Average ± SD of 3 independent experiments is reported.

Figure 2. Resistance to entrectinib in xenopatient and CRC cell models carrying *NTRK1* translocations. (A) Bioptic specimen obtained from a thin needle biopsy of a patient with metastatic colorectal cancer harboring an *LMNA-NTRK1* rearrangement was first implanted subcutaneously in an immunocompromised mouse and then expanded in multiple mice upon successful engraftment. Mice were treated with dosage levels and schedules (60mg/kg, 4 days/week) that yielded clinically relevant exposure achievable in the patients. After 3 weeks of treatment a mouse (#4) in the treated arm relapsed. Blue and red lines indicate vehicle and entrectinib treated mice, respectively. **(B)** Proliferation assay of KM12 (carrying an *TPM3-NTRK1* rearrangement) R1 cells made resistant to low dose entrectinib (300nM). Cell viability was assessed by measuring ATP content after 5 days of treatment. Sanger sequencing electropherogram of KM12 R1 shows *NTRK1* p.G667C mutation. **(C)** Proliferation assay of KM12 (carrying an *TPM3-NTRK1* rearrangement) R2 cells made resistant to a high dose of entrectinib (2μM). Cell viability was assessed by measuring ATP content after 5 days of treatment. Sanger sequencing electropherogram of KM12 R2 shows an *NTRK1* p.G595R mutation.

Figure 3. 3D modeling and homology alignment of *NTRK1* p.G595 and p.G667 variants

(A-C) Modeled binding mode of entrectinib with wildtype TRKA **(A)**, TRKA p.G595R **(B)** and TRKA p.G667C **(C).** G595R and G667C mutants create steric hindrance directly with entrectinib, making it a much weaker binder with both mutants than the wild type. The alignments of amino acid sequences

show that *NTRK1* mutation p.G595 **(D)** and p.G667 **(E)** are conserved among 6 clinically relevant tyrosine kinases listed in the figure. Both alterations are located in a residue homologous to amino acids changes involved in acquired resistance to therapies targeting other tyrosine kinases.

Figure 4. Biochemical and pharmacological characterization of xenopatient derived CRC cells.

(A) CRC cells were established from a vehicle treated xenopatient (sensitive to entrectinib) and from the tumor grown in xenopatient #4 that became resistant to entrectinib treatment *in vivo*. **(B)** Sanger sequencing electropherogram shows *LMNA-NTRK1* genetic rearrangements in both xenopatient-derived cell lines. **(C)** Cells derived from the xenopatient that developed resistance to entrectinib display *NTRK1* p.G595R mutation. **(D)** Drug proliferation assay of *LMNA-NTRK1* rearranged CRC cells. Entrectinib sensitive cells established from vehicle treated xenopatient are indicated with black line; entrectinib resistant cells established from resistant xenopatient are indicated with red line. Cell viability was assessed by measuring ATP content after 5 days of treatment**. (E)** Sensitive and resistant xenopatient-derived cells were treated with 1 μM entrectinib for 16h; after that, protein lysates were analyzed by western blot. **(F)** Sensitive and resistant xenopatient-derived cells were treated with 1 μM entrectinib for 48h; after that, protein lysates were analyzed by western blot. **(G)** RNAi knockdown of WT *NTRK1* in xenopatient derived sensitive cells and mutated *NTRK1* in xenopatient derived resistant cells induces apoptosis as shown by cleaved PARP. Protein lysates were

analyzed by western blot 3 days after transfection with NTRK1-specific pooled siRNAs, scrambled siRNA, or transfection reagent (mock).

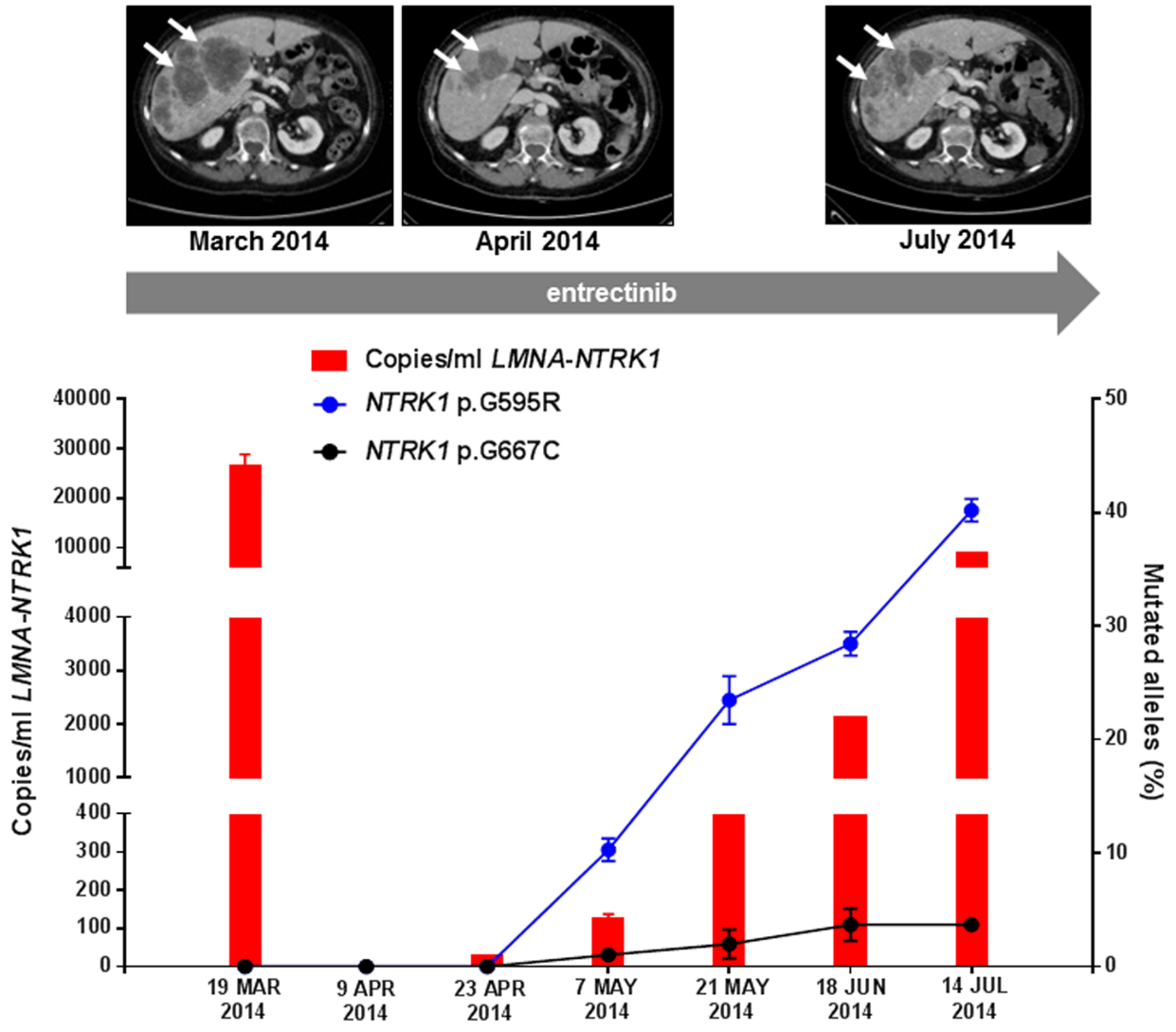

Russo et al_Figure 1

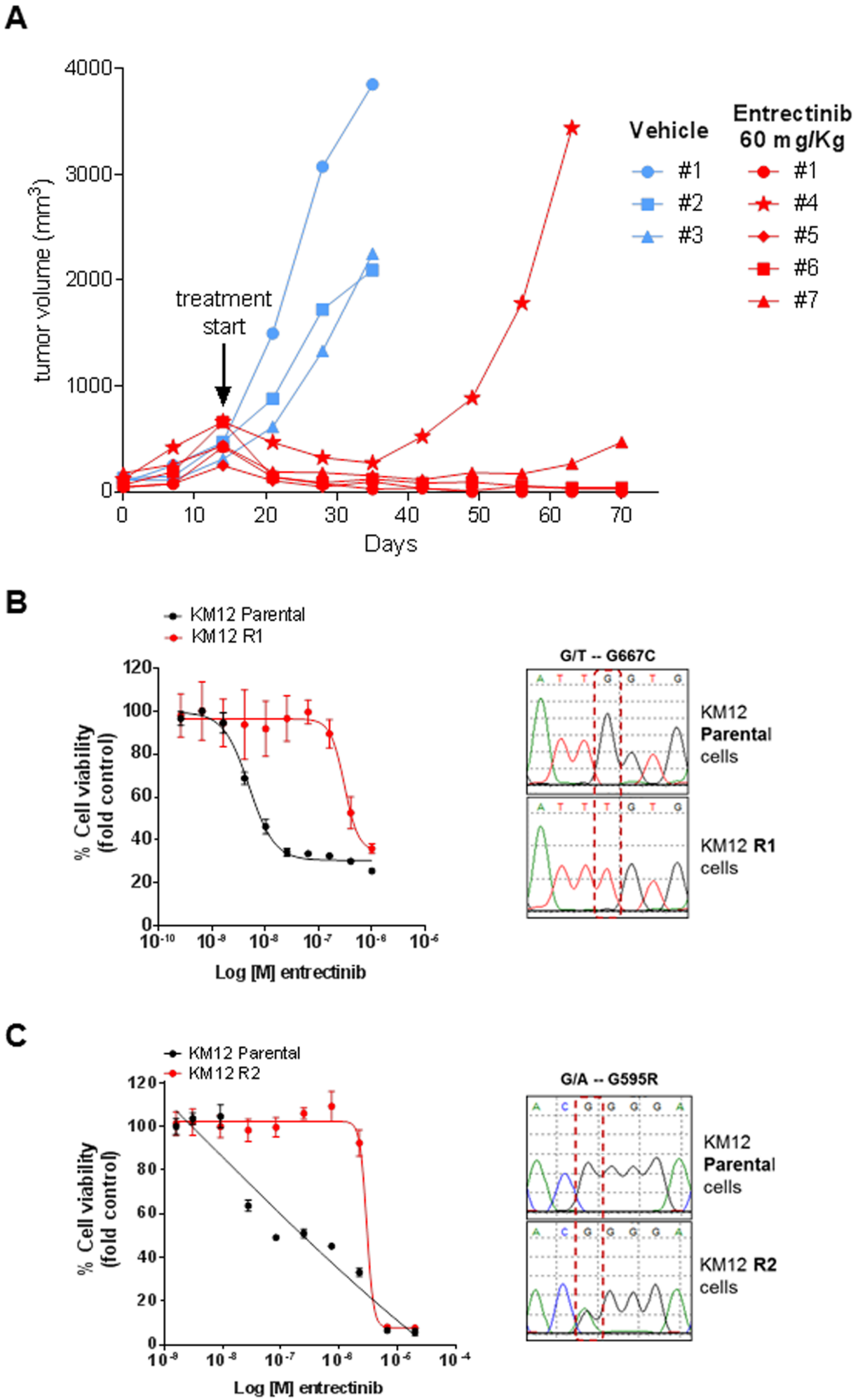

Russo et al_Figure 2

A

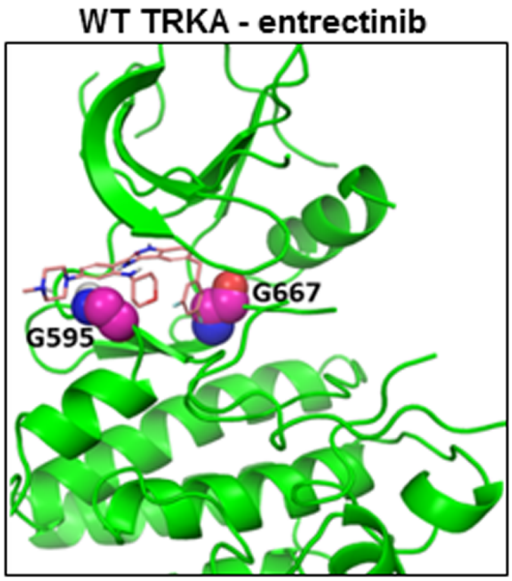

B

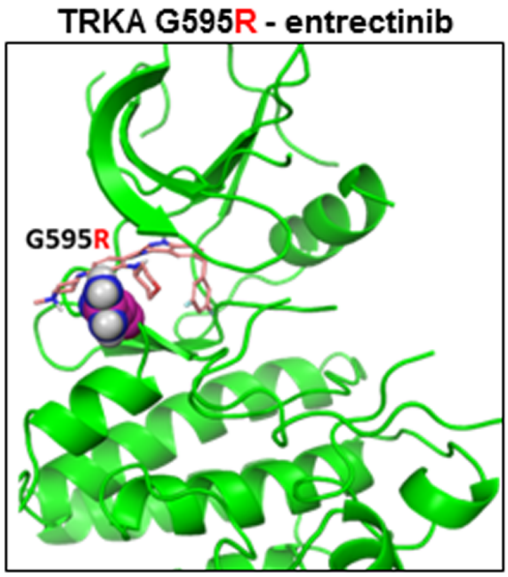

C

D

Gene	Codon	Mutation at resistance	Tissue of detection	Associated with Resistance to
NTRK1	595	p.G595R	Colon	Entrectinib
ALK	1202	p.G1202R	Lung	Crizotinib/Ceritinib
ROS1	2032	p.G2032R	Lung	Crizotinib
EGFR	796	p.G796A/R	Lung	Erlotinib/Gefitnib

E

Gene	Codon	Mutation at resistance	Tissue of detection	Associated with Resistance to
NTRK1	667	p.G667C	Colon	Entrectinib
ALK	1269	p.G1269A	Lung	Crizotinib
ROS1	2101	p.G2101A	Lung	Crizotinib
EGFR	854	p.T854A	Lung	Erlotinib/Gefitnib
KIT	809	p.C809G	GIST	Imatinib

Russo et al_Figure 3

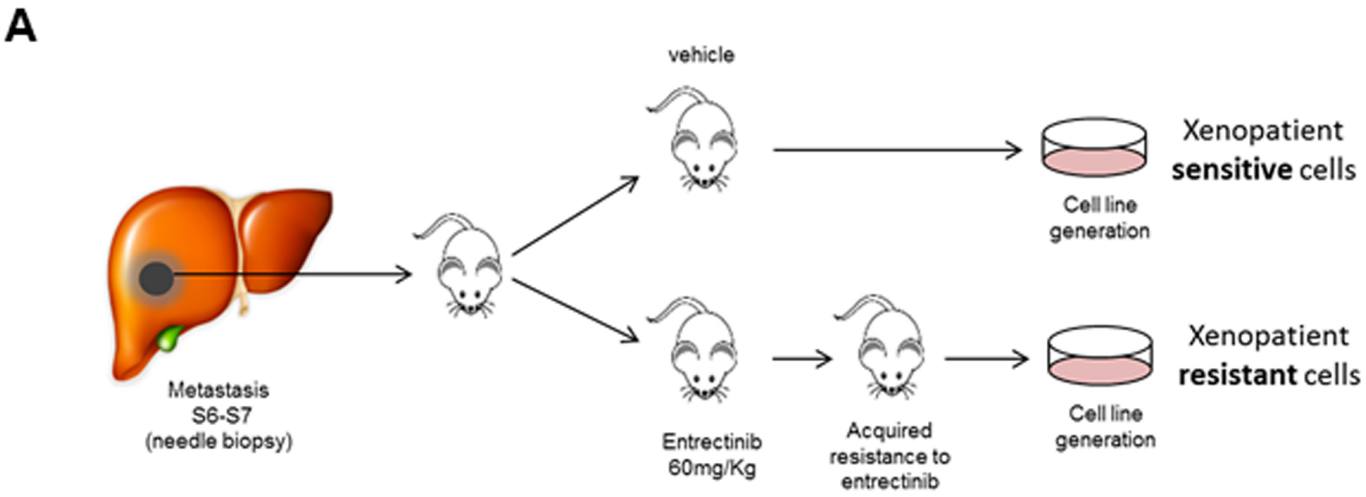

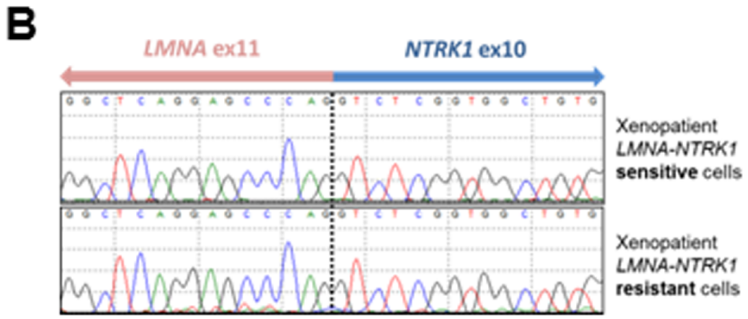

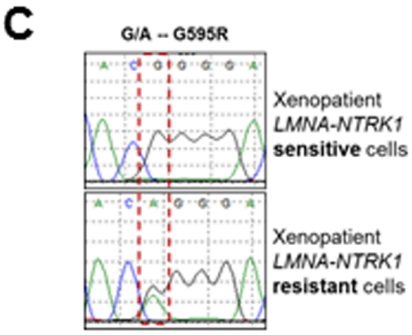

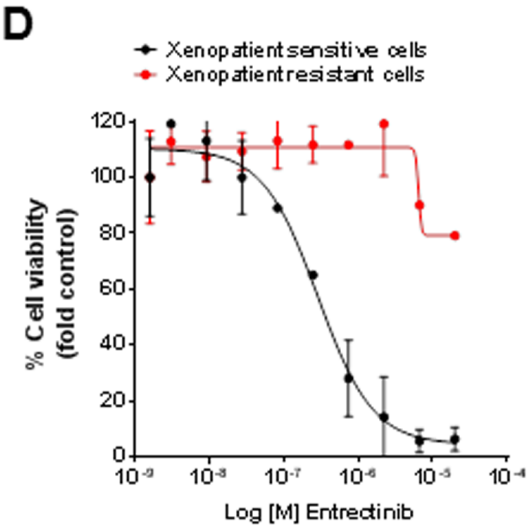

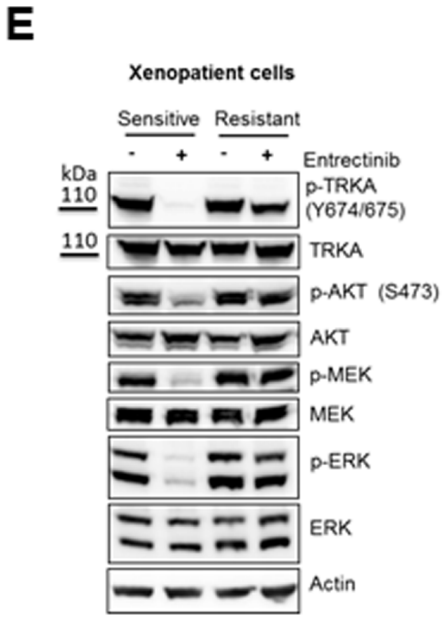

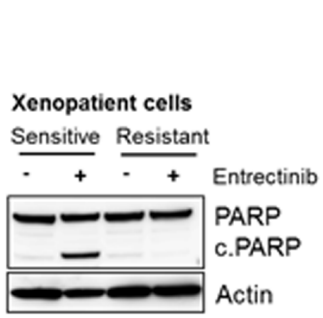

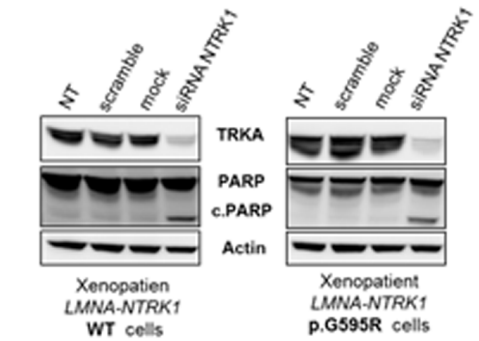

Russo et al_Figure 4

Acquired resistance to the TRK inhibitor entrectinib in colorectal cancer

Mariangela Russo, Sandra Misale, Ge Wei, Giulia Siravegna, Giovanni Crisafulli, Luca Lazzari, Giorgio Corti, Giuseppe Rospo, Luca Novara, Benedetta Mussolin, Alice Bartolini, Nicholas Cam, Roopal Patel, Shunqi Yan, Robert Shoemaker, Robert Wild,Federica Di Nicolantonio, Andrea Sartore Bianchi, Gang Li, Salvatore Siena, Alberto Bardelli

Supplementary Material and Methods

Cell culture and generation of resistant cells

KM12 cells were cultured in RPMI medium (Invitrogen) supplemented with 10% FBS, 2 mM L-glutamine, antibiotics (100 U/mL penicillin and 100 mg/mL streptomycin) and grown in a 37°C and 5% CO_2 air incubator. KM12 entrectinib-resistant derivatives were obtained by exposing cells to a chronic acute dose of 2 μM (named R2) or to escalating doses of entrectinib (named R1) until resistant derivatives emerged. Ba/F3-ETV6-TRKA cells (kind gift from Nerviano Medical Sciences) were cultured in RPMI medium (Invitrogen) supplemented with 10% FBS and antibiotics (100 U/mL penicillin and 100 mg/mL streptomycin) and grown in a 37°C and 5% CO2 air incubator. Ba/F3-ETV6-TRKA cells were treated with 30-100 nM of entrectinib initially in duplicates. The viability of Ba/F3-ETV6-TRKA cells was monitored for two to three weeks after initial treatment until the resistant populations emerged.

Xenopatient

The patient was a 75 year-old woman with metastatic CRC progressing without having had any objective response to standard previous therapies, presenting with an intact primary colon tumor, peritoneal carcinomatosis and liver metastases in segments 7 and 5 of 9.0

cm and 8.5 cm, respectively, and a right adrenal gland deposit of 2.2 cm. The primary tumor biopsied in August 2013 was colon adenocarcinoma and a liver biopsy was performed prior to provision of informed consent for molecular screening of actionable targets on March 2014. An immunohistochemical (IHC) screening ad hoc for ALK/ROS-1/TRKA abnormalities was performed within the ALKA phase 1 clinical trial. The liver biopsy was subcutaneously implanted in 8-week-old NOD-SCID mouse (from Charles River Laboratory) according to a study protocol approved by Ethical Committee at Ospedale Niguarda Ca ' Granda, Milano, Italy. The patient's tumor biopsy sample took about 1 month to engraft, after that the tumor was passaged and expanded for one generation until production of two cohorts. These were randomized according to average tumor size of 400 cubic millimeters and treated with vehicle alone (3 mice), and entrectinib (5 mice). Treatments schedule was based on oral gavage at 60 mg/kg/day for four days/week (Monday to Thursday, as usual patients' administration of the ALKA phase 1 clinical trial. Of note, continuous daily dosing is now considered the preferred schedule for entrectinib). Caliper measurements were taken once a week. Entrectinib was suspended in distilled sterile water containing 0.5% methylcellulose (Sigma Aldrich) and 1% Tween-80 (Sigma Aldrich). All animal procedures were approved by the Ethical Commission of the Institute for Cancer Research and Treatment (IRCC) and by the Italian Ministry of Health.

Drug proliferation assay

CRC cell lines were seeded at different densities (3-5 x10^3 cells/well) in 100 µl complete growth medium in 96-well plastic culture plates at day 0. The following day, serial dilutions of entrectinib were added to the cells in serum-free medium, while DMSO-only treated cells were included as controls. Plates were incubated at 37°C in 5% CO_2 for 3-5 days, after which cell viability was assessed by measuring ATP content through Cell Titer-Glo® Luminescent Cell Viability assay (Promega). Luminescence was measured by Perkin

Elmer Victor X4 or BMG ClairoStar plate reader. IC50s were determined by 4-parameter curve fit with variable slope (Prism6).

Western blotting analysis

Prior to biochemical analysis, all cells were grown in their specific media supplemented with 10% FBS. Cells were treated with indicated concentrations of entrectinib for 16 or 72 hours. Total cellular proteins were extracted by solubilizing the cells in EB buffer (50 mM Hepes pH 7.4, 150 mMNaCl, 1% Triton X-100, 10% glycerol, 5 mM EDTA, 2 mM EGTA; all reagents were from Sigma-Aldrich, except for Triton X-100 from Fluka) in the presence of 1 mM sodium orthovanadate, 100 mM sodium fluoride and a mixture of protease sinhibitors. Extracts were clarified by centrifugation and normalized with the BCA Protein Assay Reagent kit (Thermo). Western blot detection was performed with enhanced chemiluminescence system (GE Healthcare) and peroxidase conjugated secondary antibodies (Amersham). The following primary antibodies were used for western blotting (all from Cell Signaling Technology, except where indicated): anti-phospho TRKA (Tyr674/675) (SantaCruz); anti-TRK (SantaCruz); anti-phospho AKT (Ser473); anti-AKT; anti-phospho-p44/42 ERK (Thr202/Tyr204); anti-p44/42 ERK; anti-phospho-MEK1/2 (Ser217/221), anti-MEK1/2; anti-PARP; anti-actin (Millipore).

siRNA screening

The siRNA targeting reagents were purchased from Dharmacon, as a SMARTpool of four distinct siRNA species targeting different sequences of the TRKA transcript. Cell lines were grown and transfected with SMARTpool siRNAs using RNAiMAX (Invitrogen) transfection reagents following manufacturer's instructions. Briefly RNAi screening conditions were as follows: on day one siRNA were distributed in each well of a 6-well plate at final concentration of 20 nmol/L. Transfection reagent was diluted in OptiMEM and

aliquoted at 250µl/well; after 20 minutes of incubation, 2ml in media without antibiotics were added to each well. After 3 days, total cellular proteins were extracted to perform western blot analysis. Each plate included the following controls: mock control (transfection lipid only), scramble (AllStars, Qiagen) as negative control.

Plasma Samples Collection

At least 10 mL of whole blood were collected by blood draw using EDTA as anticoagulant. Plasma was separated within 5 hours through 2 different centrifugation steps (the first at room temperature for 10 minutes at 1,600 × g and the second at 3,000 × g for the same time and temperature), obtaining up to 3 mL of plasma. Plasma was stored at -80°C until ctDNA extraction.

ctDNA isolation and genome equivalents quantification (GE/ml plasma)

ctDNA was extracted from plasma using the QIAamp Circulating Nucleic Acid Kit (QIAGEN) according to the manufacturer's instructions. 6 µl of ctDNA were used as template for each reaction. All samples were analyzed in triplicate. PCR reactions were performed using 10 µl final volume containing 5 µl GoTaq®qPCR Master Mix, 2X with CXR Reference Dye (Promega) and LINE-1 [12,5µmol] forward and reverse primers. DNA at known concentrations was also used to build the standard curve. Primer sequences are listed in Supplementary Table S5.

3-Dimensional modelling of TRKA

The binding mode of entrectinib with wild type TRKA was obtained using Glide docking implemented in Maestro (Maestro Release 2015-1, Schrodinger, Inc, New York, NYC, 2015). Receptor coordinates were downloaded from PDB (PDB code: 4PMT) and properly prepared by adding protons, sampling water orientations and finally full energy

minimization. Both p.G595R and p.G667C mutated models were built with Maestro and subsequently subjected to energy minimization.

Supplementary Figures and Tables

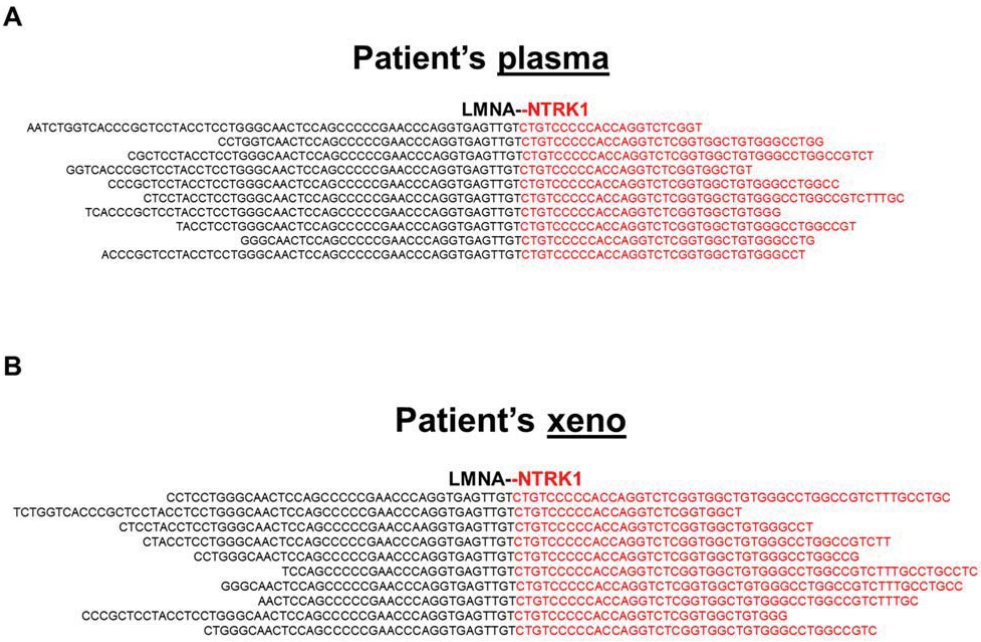

Supplementary Figure S1. *LMNA-NTRK1* genetic rearrangement detected in patient's plasma and xeno. NGS analysis using the IRCC-TARGET panel retrieved an in-frame gene fusion event between exon 11 of the *LMNA* gene and the exon 10 of the *NTRK1* gene in patient's plasma **(A)** and xeno **(B)**.

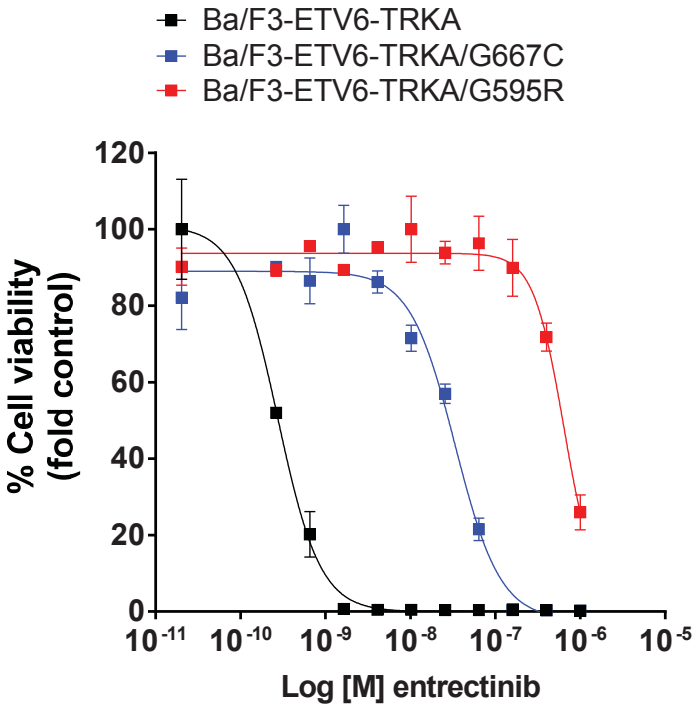

Supplementary Figure S2. Acquisition of mutations in the TRKA kinase domain drives secondary resistance to entrectinib in Ba/F3 TRKA WT cells. Proliferation assay of Ba/F3-ETV6-TRKA WT, Ba/F3-ETV6-TRKA G667C and Ba/F3-ETV6-TRKA G595R cells. Cell viability was assessed by measuring ATP content after 3 days of treatment with the indicated concentrations of entrectinib.

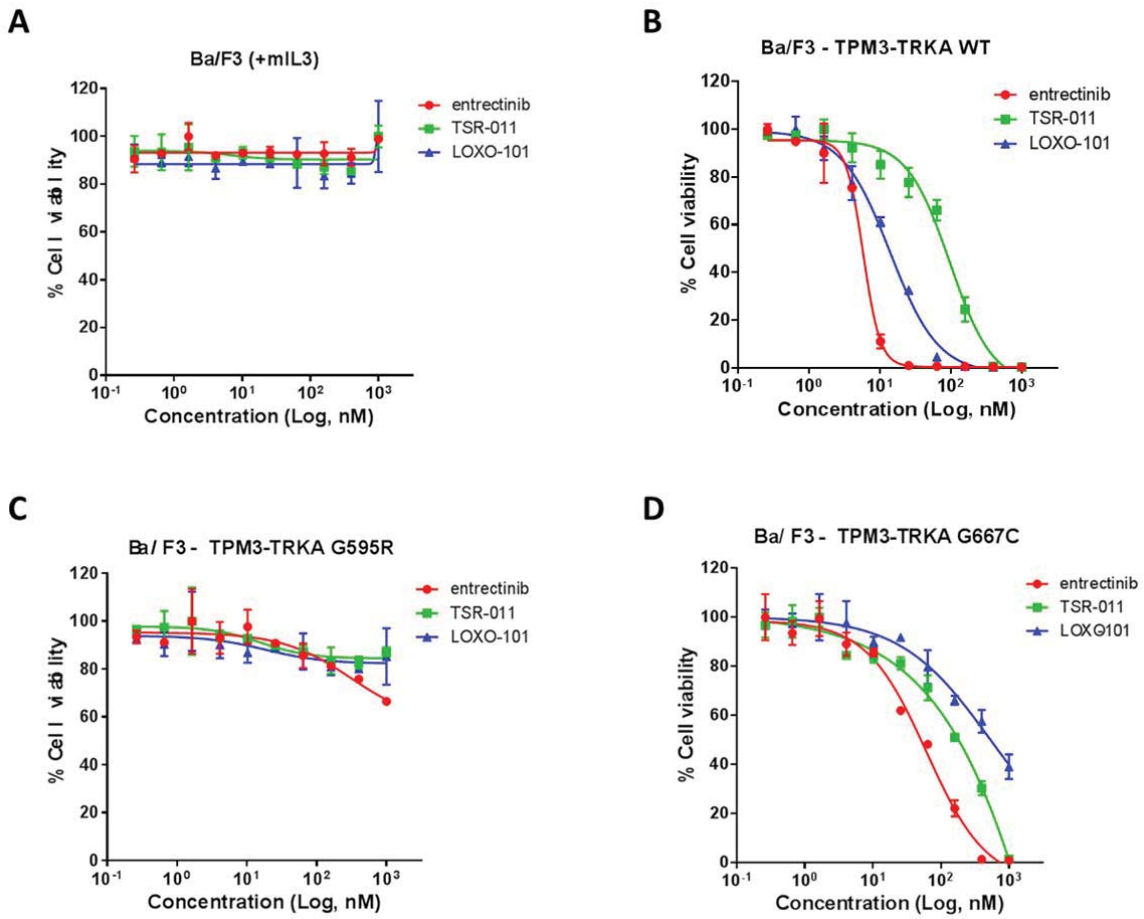

Supplementary Figure S3. *NTRK1* mutations confer resistance to TRKA inhibition. Proliferation assay of Ba/F3 **(A)**, Ba/F3-TPM3-TRKA WT**(B)**, Ba/F3-TPM3-TRKA G595R **(C)** and Ba/F3-TPM3-TRKA G667C **(D)**. Cell viability was assessed by measuring ATP content after 3 days of treatment with indicated concentrations of entrectinib, LOXO-101 or TSR-011.

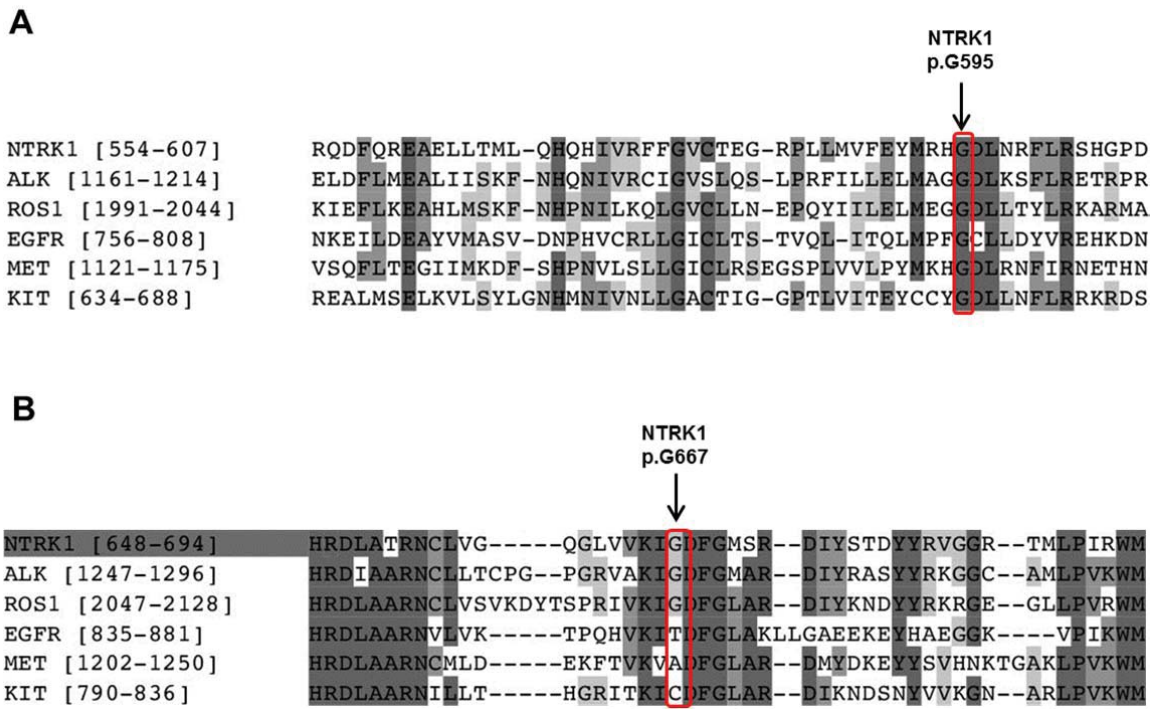

Supplementary Figure S4. Homology alignment of *NTRK1* p.G595 and p.G667 variants. The alignments of amino acid sequences show that *NTRK1* mutation p.G595 **(A)** and p.G667 **(B)** are conserved among 6 clinically relevant tyrosine kinases listed in the figure. Conserved residues among the all aligned kinase domains are highlighted in grey scale colors depending on their level of identity (dark grey: high identity; white: low identity).

Supplementary Tables

	Plasma baseline			Plasma at resistance			Mouse Tumor (Vehicle)			Mouse Tumor (Resistance)		
Variant	MUT reads	WT reads	Fractional abundance (%)	MUT reads	WT reads	Fractional abundance (%)	MUT reads	WT reads	Fractional abundance (%)	MUT reads	WT reads	Fractional abundance (%)
NTRK1 **p.G595R**	0	440	0	99	311	24.0	0	288	0	107	196	35.3
NTRK1 **p.G667C**	0	301	0	11	261	4.0	0	253	0	0	300	0

Supplementary Table S1. NGS analysis of *NTRK1* gene in patient's plasma and xeno. The table lists the wild type (WT) and mutated (MUT) reads and fractional abundance (%) of mutations detected by NGS (IRCC-TARGET panel) analysis from plasma collected at baseline and resistance to entrectinib and from tumors grown in resistant and vehicle mice.

	COSMIC occurrence	gene	variant effect	variant	WT reads	MUT reads	Fractional abundance (%)
ctDNA at entrectinib resistance	**0**	***NTRK1***	**nonsynonymous**	**p.G595R**	**311**	**99**	**24,0**
	0	***NTRK1***	**nonsynonymous**	**p.G667C**	**262**	**11**	**4,0**
	0	*NPM1*	nonsynonymous	p.P71A	880	24	2,7
	0	*PMS1*	nonsynonymous	p.S253L	587	14	2,3
	0	*PIK3CD*	nonsynonymous	p.V538I	649	15	2,3
	1	*BRCA1*	nonsynonymous	p.K1254T	1517	33	2,1
	0	*ROS1*	nonsynonymous	p.P1154H	462	10	2,1
	0	*MAPK12*	nonsynonymous	p.G157D	806	17	2,1
	0	*TSHR*	nonsynonymous	p.D276A	1437	23	1,6
Tumor derived from resistant Xeno	1	*STK11*	nonsynonymous	p.G242E	118	146	55,3
	0	*ATM*	nonsynonymous	p.E2257D	231	212	47,9
	0	***NTRK1***	**nonsynonymous**	**p.G595R**	**196**	**107**	**35,3**
	4	*FLT3*	nonsynonymous	p.A627T	1340	354	20,9
	0	*ERCC5*	nonsynonymous	p.G14E	1159	293	20,2
	0	*FGFR3*	stopgain	p.Q602*	469	13	2,7
Cells derived from Resistant Xeno	**0**	***NTRK1***	**nonsynonymous**	**p.G595R**	**213**	**104**	**32,7**
	0	*TSHR*	nonsynonymous	p.K565E	771	31	3,9
	0	*POLD1*	nonsynonymous	p.C991Y	399	16	3,8
	1	*BLM*	nonsynonymous	p.T298M	661	16	2,4
	2	*NOTCH2*	nonsynonymous	p.R1630H	760	17	2,2
	0	*FGFR3*	stopgain	p.Q602*	558	11	1,9
	0	*PTPN11*	nonsynonymous	p.S234R	805	13	1,6

Supplementary Table S2. NGS analysis of patient's derived samples. The table shows mutations identified using the IRCC-TARGET-NGS panel analysis in the patient's plasma ctDNA (obtained at entrectinib resistance), the resistant xeno and cells established from resistant xeno. To uncover somatic mutations, we compared each resistant sample to its sensitive counterpart as previously described (Siravegna et al, Nat Med 2015), and identified base-pair mismatches (Fisher's Test) with fractional abundance above 1.5%. Mutations were then called only when supported by a 5% statistical significance and their occurrence was checked in the COSMIC database. Mutations were annotated (from left to right) according to gene name, the variant effect (synonymous, non-synonymous, stop-loss/gain), protein change (variant), number of wildtype (WT) or mutated (MUT) reads and the allelic frequencies (fractional abundance). Every somatic mutation was validated by visual examination using BAM files.

GE/ml plasma	Sample ID	Target	ddPCR Copies/ml Translocation	ddPCR Mut events	ddPCR WT events	Poisson Corrected (95% C.I.) Fractional Abundance (%)
32211268	19 MAR 2014	*LMNA-NTRK1*	26460	--	--	--
		NTRK1 p.G595R	--	0	4047	negative
		NTRK1 p.G667C	--	0	5568	negative
702720	9 APR 2014	*LMNA-NTRK1*	0	--	--	--
		NTRK1 p.G595R	--	0	131	negative
		NTRK1 p.G667C	--	0	173	negative
493986	23 APR 2014	*LMNA-NTRK1*	13	--	--	--
		NTRK1 p.G595R	--	0	130	negative
		NTRK1 p.G667C	--	0	86	negative
379045	7 MAY 2014	*LMNA-NTRK1*	123	--	--	--
		NTRK1 p.G595R	--	15	129	10.3 (15.05-5.05)
		NTRK1 p.G667C	--	3	284	1.05 (2.9-0)
504662	21 MAY 2014	*LMNA-NTRK1*	399	--	--	--
		NTRK1 p.G595R	--	43	141	23.5 (30-17.5)
		NTRK1 p.G667C	--	8	374	2 (4.05-0.25)
2708390	18 JUN 2014	*LMNA-NTRK1*	2107	--	--	--
		NTRK1 p.G595R	--	180	456	28.45 (31.9-24.95)
		NTRK1 p.G667C	--	19	486	3.7 (5.4-2.05)
9274704	14 JUL 2014	*LMNA-NTRK1*	8610	--	--	--
		NTRK1 p.G595R	--	718	1084	40.2 (42.4-38.05)
		NTRK1 p.G667C	--	74	2010	3.7 (4.5-2.95)

Supplementary Table S3. Summary of serial ctDNA analyses. Circulating tumor DNA (ctDNA) was isolated from serial blood draws collected before initiation of entrectinib (19 MAR 2014), and until treatment was terminated (14 JUL 2014). Each time point was analyzed by droplet digital PCR (ddPCR). The number of Genome Equivalents (GE), mutated (MUT) and wild type (WT) events and fractional abundance (%) are listed.

IC50 (nM)	Ba/F3-TPM3-TRKA WT	Ba/F3-TPM3-TRKA G595R	Ba/F3-TPM3-TRKA G667C	Ba/F3 (+mIL3)
entrectinib	5.9	>1000	61.53	>1000
TSR-011	97.3	>1000	>1000	>1000
LOXO-101	14.0	>1000	524.2	>1000

Supplementary Table S4. The p.G595R and p.G667C mutations confer resistance to multiple TRK inhibitors. Ba/F3, Ba/F3-TPM3-TRKA WT, Ba/F3-TPM3-TRKA G595R and Ba/F3-TPM3-TRKA G667C were treated with indicated TRK inhibitors for 3 days. IC50 values, determined by 4-parameter curve fit with variable slope, are listed in the Table.

	NTRK1 p.G667C ddPCR custom probes	*NTRK1* p.G595R ddPCR custom probes	*LMNA-NTRK1* fusion ddPCR custom probes
Forward Sequence	TCTAGTGGGCCAGGG	CCTGCTCATGGTCTTTGA	TGGGCAACTCCAGCCC
Reverse Sequence	GCTGTAGATATCCCTGCT	CGGAGGAAGCGGTTG	CACAGCCACCGAGACCT
MUT Probe Sequence (FAM)	AAGATTTGTGATTTTGGCATG	CGGCACAGGGACCT	CCCAGGTGAGTTGTCTGTCCC
WT Probe Sequence (HEX)	AAGATTGGTGATTTTGGCAT	CGGCACGGGGACC	

Supplementary Table S5. *NTRK1* p. G595R, p.G667C and *LMNA-NTRK1* fusion probes for ddPCR. Primers and probes used for ddPCR analysis are listed in the Table.